

High-temperature hydrogen attack of carbon steel

D. ELIEZER

Materials Engineering Department, Ben Gurion University of the Negev, Beer Sheva, Israel

A systematic study was made of the mechanical properties and the microscopic fracture processes associated with hydrogen attack of SAE 1020 carbon steel in a well-controlled, high-temperature, high-purity hydrogen environment. Exposure to a hydrogen pressure of 3.5 MN m^{-2} and temperature 525°C was found to progressively degrade room-temperature tensile properties with increasing exposure time. After exposure for 360 h the yield and ultimate strength were reduced by 58% and 40% of the unexposed values, respectively, and the elongation-at-fracture was reduced to less than 2%. Sub-critical crack growth tests under conditions of static loading were conducted at various temperatures and hydrogen pressures. It was observed that blisters and tears were not evenly distributed on the hydrogen-attacked specimens, but their distributions were, instead, very dependent on specimen thickness. During the hydrogen attack, tears form and undergo crack growth as a result of the formation and accumulation of methane under high pressure at the weak interfaces such as at the inclusion-matrix or ferrite-pearlite bands. If the tear is located close to the surface it bulges and forms into a blister. Tears and blisters may lead to accelerated failure by hydrogen attack.

1. Introduction

A number of energy related systems, particularly advanced energy conversion systems such as coal gasifiers and fossil fuel processors, involve the containment of hydrogen at high temperatures and pressures. Such high temperature and pressure hydrogen may cause a loss of strength, swelling and ultimately fracture in such a steel containment vessel. Hydrogen attack occurs as a result of atomic hydrogen diffusing into the steel and combining with carbon in solution to form methane which, because of its insolubility in steel, remains trapped internally as bubbles [1-6]. The methane, unable to diffuse through the steel, accumulates in pre-existing sub-microscopic defects (voids) and develops high internal pressures that cause the growth and coalescence of these voids. The voids on the grain boundaries eventually coalesce into fissures producing extensive intergranular fissuring leading to the failure of the steel.

The temperature range of hydrogen attack of carbon steels extends from about 160°C to 540°C .

This temperature range coincides with the range of service temperatures of steels in petroleum refining and other equipment [3,4]. The usual means of predicting the behaviour of materials in high pressure, high temperature hydrogen is Nelson curves [7]. These curves delineate the safe and unsafe hydrogen pressure-temperature regimes for carbon and alloy steel in a purely empirical manner. These diagrams are used extensively in the design of systems that use hydrogen and are adjusted to more conservative limits as unexpected new failures are reported. The data collected in the Nelson curve come almost exclusively from experience gained in the oil and petrochemical industries and may not be directly applicable to other areas such as design for coal gasification systems. Coal conversion processes offer a partial solution to the problem of meeting an increasing demand for energy supplies. A common requirement for all these processes is the need for pressure vessels to operate continuously and safely under conditions of high temperature, high pressure and

TABLE I Chemical analysis of SAE 1020 carbon steel

Element (wt %)										
Mn	Si	C	Cu	Si	Cr	Mo	Ni	P	Co	Sn
0.58	0.25	0.19	0.08	0.022	0.02	0.02	0.02	0.014	0.009	0.008

potentially hostile environments. These hostile environments in combination with the high pressures and temperatures could have a pronounced detrimental effect on the rate at which cracks could initiate and propagate in the pressure vessels, ultimately resulting in a structural failure.

The objective of the present study is to better understand the period of rapid high-temperature hydrogen attack through its influence on the mechanical behaviour of a plain carbon steel, including hydrogen attack-induced sub-critical crack growth under sustained load conditions. The microscopic fracture processes associated with hydrogen attack in a well-controlled high-temperature, high-purity hydrogen environment are discussed.

2. Experimental procedure

The material used in this investigation was commercially produced SAE 1020 steel plate of thickness 12.5 mm. The chemical composition of the material is shown in Table I. Tensile specimens having a gauge length of 28 mm and a thickness of 2.5 mm were cut with their long axis perpendicular to the direction of rolling.

Environmental exposures were conducted in an all-metal, sealed, tubular stainless steel chamber surrounded by a resistance-heated tube furnace. Furnace temperature was automatically controlled by a set-point temperature controller and a stepless power transformer.

Prior to exposure to the test environment, the following procedure was employed to remove the oxide from the surface of the specimens: (a) the chamber was first evacuated to a pressure of less than 0.6 N m^{-2} , (b) charged at room temperature with hydrogen to a pressure of 3.5 MN m^{-2} , (c) evacuated, (d) brought up to 300° C , (e) charged with 690 kN m^{-2} hydrogen for 10 h, (f) evacuated, (g) raised to 525° C , and (h) given the final charge of the test environment to the desired pressure.

The hydrogen was of laboratory grade that initially contained less than 100 ppm of active impurity gases (O_2 , H_2O , N_2), as determined by mass spectrometric methods; the hydrogen was

additionally purified by passing it slowly through a liquid-nitrogen cooled coil.

Specimen temperature was maintained to within $\pm 5^\circ \text{ C}$ during environmental exposure. Following exposure, the chamber containing the specimens was reduced in temperature to 400° C , evacuated for 60 min, and furnace-cooled to room temperature. This termination procedure reduced the amount of hydrogen dissolved in the metal, while retaining the methane which was formed during environmental exposure.

Room-temperature tensile tests were conducted at a fixed displacement rate of $1 \times 10^{-2} \text{ cm sec}^{-1}$. The fracture surfaces of all failed specimens were observed by scanning electron microscopy.

Sub-critical crack growth tests were conducted in a high-purity hydrogen atmosphere at various temperatures ranging from 375 to 525° C and for times ranging from 10 to 30 days. Wedge-opening loaded (WOL) specimens 1.25 cm thick, fracture mechanics type, were cut from the SAE 1020 plate so that the crack would propagate in the rolling direction on a plane normal to the transverse rolling direction. In these tests, the displacement was held at a known constant value during a test and load levels and changes in load could be related to specimen compliance. In accordance with [8], specimens with fatigue pre-cracked in air and wedges were driven into the initial machined notches to produce a fixed crack-opening displacement (COD). After removal from the furnace, the specimens were air-cooled and then reloaded to determine the actual final load. Specimens were fatigue cracked after testing in order to protect the region that was hydrogen attacked, and were then failed by overload. The

TABLE II The experimental matrix for the study of hydrogen attack effects on sub-critical crack growth for a pressure of 500 psi and duration 10 days

Temperature, T ($^\circ \text{ C}$)	K ($\text{MN m}^{-3/2}$)			
	12	24	36	48
525	×	×	×	×
450	×	×	×	×
375	×	×	×	×

TABLE III The experimental matrix for the study of hydrogen attack effects on sub-critical crack growth for a pressure of 500 psi and a temperature of 450° C

Time of exposure, <i>t</i> (days)	<i>K</i> (MN m ⁻²)			
	12	24	36	48
10	x	x	x	x
20	x	x	x	x
30	x	x	x	x

experimental matrix for the study of hydrogen attack effects on sub-critical crack growth is shown in Tables II and III.

All samples were sectioned and polished to examine the effect of hydrogen attack upon the microstructure using optical and scanning electron microscopy.

3. Results and discussion

A high-purity hydrogen environment at 525° C was found to significantly degrade the tensile properties of SAE 1020 steel after as little as 120 h of exposure, the shortest exposure time of this study. Fig. 1 is a summary of the tensile curves observed at room temperature for a specimen exposed at 525° C to a vacuum environment and a specimen exposed at 525° C to a hydrogen environment for 360 h. As shown in Fig. 1, yield strength, ultimate tensile strength, and elongation-at-fracture are all reduced as a result of exposure to the high-pressure hydrogen environment. As can be seen, exposure to hydrogen for 360 h results in a 58% reduction in the yield strength a

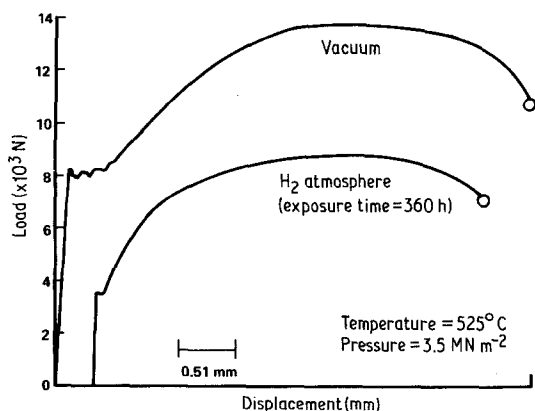


Figure 1 A summary of tensile curves observed at room temperature for 1020 steel for a sample exposed to a vacuum environment at 525° C and a sample exposed to a hydrogen environment for 360 h at 525° C.

40% reduction in the ultimate tensile strength and elongation-at-fracture is reduced to less than 2%.

Examination of the fracture surfaces of the specimens exposed to the hydrogen environment indicates massive regions of microvoid coalescence producing ductile rupture (Fig. 2). The formation of microvoids was often associated with particles which were identified as manganese sulphide particles with some indication of aluminium and silicon [9]. Void formation during hydrogen attack around manganese particles has been previously observed [10, 11]. Pisko *et al.* [12] found that hydrogen attack started with the nucleation and growth of myriad small bubbles on a minority of the ferrite-pearlite or ferrite-ferrite boundaries.

Sub-critical crack growth studies under conditions of static loading were conducted, as described in the experimental matrix (Table II). The results show that there was essentially no crack growth under the aforementioned testing conditions. A possible explanation for the lack of slow crack growth is that the tip crack of the WOL specimens is not located on grain boundaries and subsequently no methane bubbles are formed in that region. It may be significant that no slow crack growth was observed in the 1020 steel, a phenomenon which does not appear to have been reported previously.

The initial microstructure of this steel was ferrite and fine pearlite. After 120 h of exposure at 525° C in hydrogen, the structure had transformed to spheroidized carbide in a ferrite matrix. After 240 h of exposure at 525° C in hydrogen carbides could not be observed.

During this study, it was observed that blisters and tears were not evenly distributed on the exposed surfaces of the specimens, but instead were very dependent on specimen thickness. It is possible that this effect may be the result of triaxial constraint in thicker areas and lack of such constraint in the thinner areas, as suggested by [13]. An examination of the tensile specimen surface at the gauge length revealed numerous small bulges or protrusions which appear approximately like hemispherical caps (Fig. 3). These protrusions are termed "blisters". The diameters of these blisters can be as large as 2 mm and they are considerably bigger than the diameters of the approximately spherical bubbles which form at the grain boundary in the interior [11, 14]. It is interesting to note that the blisters observed

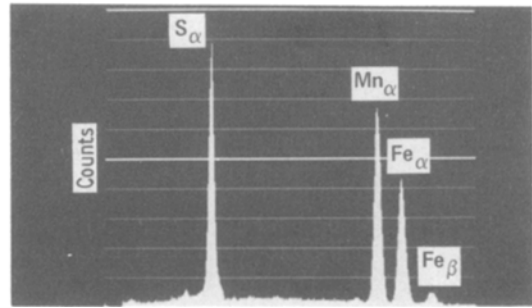
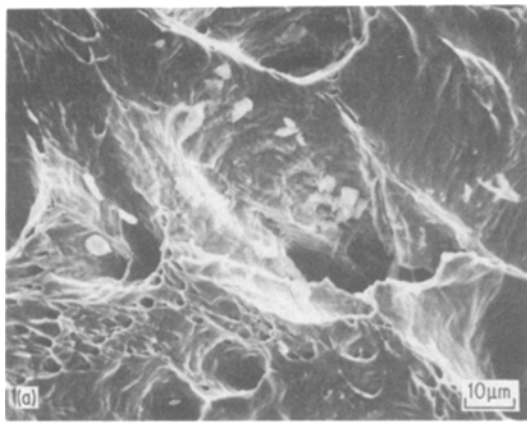


Figure 2 Scanning electron microscopy (SEM) fractograph of fracture surfaces showing (a) massive regions of microvoid coalescence producing ductile rupture, (b) electron dispersive X-ray (EDAX) analysis showing manganese sulphide particles.

on the gauge length surface are either absent or smaller and fewer on the shoulders of the tensile specimen.

Sorell and Humphries [15] report the close relationship and resemblance between blisters and fissuring in a damaged carbon steel. Once fissures begin to interconnect it becomes easier for the steel surface to bulge out and for progressive damage along the plane of the blisters. Such blistering is inevitably accompanied by extensive decarburization. A tear observed in the interior of the specimen is shown in Fig. 4. These tears are extensive at the gauge length, relatively few at the shoulder, and are not observed in the WOL specimen. It can be seen (Fig. 4) that the region close to the tear has very coarse ferrite grain structure. The preferential recrystallization and grain

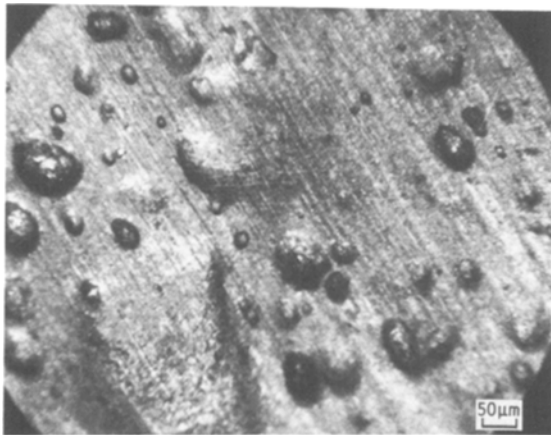


Figure 3 A typical surface of a specimen exposed to gaseous hydrogen at a pressure of 3.5 MN m^{-2} and at a temperature of 525° C for 240 h.

coarsening confirms that substantial internal pressure exists inside the tear. A typical blister observed in a partially hydrogen-attacked specimen is shown in Fig. 5. When a tear is located close to the specimen surface it bulges and produces blisters. It is proposed that during hydrogen attack of a commercial 1020 steel, tears form and undergo crack growth as a result of the formation and accumulation of methane under high pressure at the weak interfaces such as at the inclusion–matrix or the ferrite–pearlite bands. The internal pressure of methane within the tear is maintained due to the continued hydrogen attack and the tear runs along the length of the specimen leading to delamination. It should be mentioned that all the attacked specimens showed methane bubbles (of size about $2 \mu\text{m}$) along grain boundaries similar to those observed by others [11]. As exposure time increases these bubbles begin to coalesce into fissures. In the more advanced stages of hydrogen attack some of the fissures form into large tears (of about size $60 \mu\text{m}$) along the inclusion in the rolling direction. If a large tear is located close to the surface, it bulges to form a blister. The tears grow and the blisters bulge rapidly, compared to the growth of the bubbles, leading to fissuring and delamination. Therefore, tearing and blistering may lead to accelerated failure by hydrogen attack.

4. Conclusions

Hydrogen attack of SAE carbon steel from a high-purity hydrogen environment was found to be severe with the formation of numerous methane fissures, bubbles and tears and with a significant

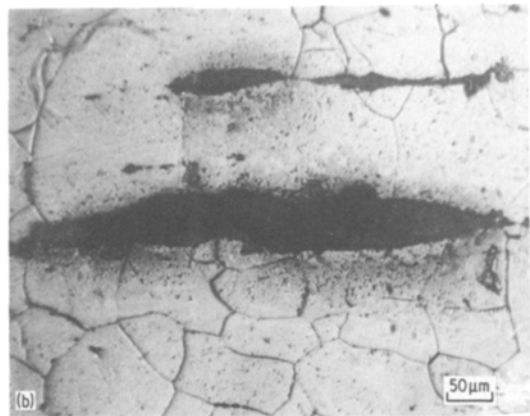
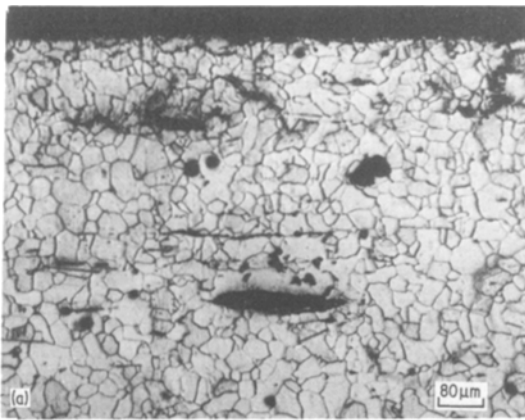


Figure 4 Tears observed in a completely decarburized specimen.

reduction in the room-temperature yield and ultimate tensile strengths.

Specimens that were fractured at room temperature after exposure to hydrogen indicate massive regions of microvoid coalescence producing ductile rupture.

Sub-critical crack growth studies under conditions of static loading at different pressures and temperatures were conducted. The results show that there was essentially no crack growth.

It was observed that blisters and tears were not evenly distributed on the hydrogen-attacked specimens, but instead their distributions were very dependent on specimen thickness. It is proposed that when a tear is large enough and is located close to the surface, it bulges and forms a blister. Tears and blisters may lead to accelerated failure by hydrogen attack.

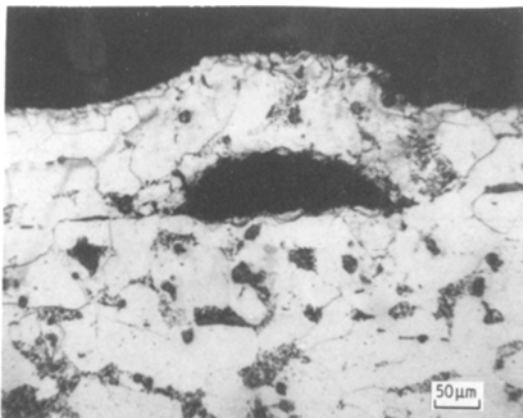


Figure 5 Tear bulges into a blister in a partially decarburized specimen.

Acknowledgment

The author acknowledges Dr H. G. Nelson for his instructive discussions.

References

1. R. E. ALLEN, R. J. JANSEN, P. C. ROSENTHAL and F. H. VITOVEC, *Proc. Amer. Petroleum Inst.* **42** (1962) 452.
2. L. C. WEINER, *Acta Metal.* **8** (1960) 52.
3. *Idem*, *Corrosion* **17** (1961) 137t.
4. H. H. PODGURSKI, *Trans. TMS-AIME* **221** (1961) 389.
5. D. A. WESTPHAL and F. J. WORZALA, "Hydrogen in Metals" edited by A. W. Thompson and I. M. Bernstein (American Society for Metals, Metals Park, Ohio, 1974).
6. P. SHEWMAN, *Met. Trans.* **7A** (1976) 279.
7. "Steels for Hydrogen Service at Elevated Temperatures and Pressures in Petroleum Refineries and Petrochemical Plants" Publication number 941 (American Petroleum Industries, New York, 1970).
8. ASTM Standard Number 399-740.
9. D. ELIEZER and H. G. NELSON, *Corrosion* **35** (1979) 17.
10. H. G. NELSON and R. D. MOORHEAD, *ASTM STP* **600** (1976) 88.
11. H. M. SHIH and H. H. JOHNSON, *Scripta Met.* **11** (1977) 151.
12. R. PISKO, M. McKIMPSON and P. SHEWMAN, *Met. Trans.* **10A** (1979) 887.
13. R. D. SISSON and J. R. TORAN, "Environmental Degradation of Engineering Materials: Hydrogen Blister Formation in Aluminum Alloys" (VPI and SU, 1977).
14. A. A. SAGUES, B. O. HALL and H. WIEDERSICH, *Scripta Met.* **12** (1978) 319.
15. G. SORELL and M. J. HUMPHRIES, *Mater. Performance* **17** (1978) 33.

Received 23 December 1980 and accepted 23 March 1981.